INSTITUT PASTEUR

Research in Microbiology 158 (2007) 187–194

www.elsevier.com/locate/resmic

Review

# Applications of fluorescence microscopy to single bacterial cells

Pablo Meyer, Jonathan Dworkin*

*Department of Microbiology, College of Physicians and Surgeons, Columbia University, 701 West 168th Street, Room 1218, New York, NY 10032, USA*

Received 14 September 2006; accepted 1 December 2006
Available online 18 January 2007

**Abstract**

Fluorescence-imaging techniques are now being applied to single bacterial cells for the determination of in vivo kinase and transcription activity, protein–protein interactions, protein localization and protein mobility. Time-lapse imaging is being used at a population level to study heterogeneities, colony morphologies and the genetic networks underlying these phenomena. We will discuss here the possibilities, advantages and limitations of such techniques, focusing on the use of green fluorescent protein and its spectral variants.


*Keywords:* Fluorescence; Green fluorescent protein (GFP); Fluorescence resonant energy transfer (FRET); Fluorescence recovery after photobleaching (FRAP); Bacteria; Microscopy; Single cell; Time lapse

## 1. Introduction

The cloning of green fluorescent protein (GFP) [32], together with significant improvements in microscopy, has greatly facilitated the development of refined imaging techniques for studying protein activity and localization in single cells. These methods were mostly developed in eukaryotic cells, but are now also being applied to bacteria. We will first describe the physical basis for techniques such as FRET (fluorescence resonant energy transfer) and FRAP (fluorescence recovery after photobleaching), then discuss and illustrate with examples some improvements and the discovery of new methods for detecting protein activity and protein interactions in single bacterial cells.

### *1.1. Time-lapse, deconvolution and confocal imaging*

Improvements in imaging acquisition systems (software and hardware) now permit the observation of live single bacterial cells under stable conditions for days [42] and even months [28]. One can now not only monitor individual cell lineages in growing colonies of bacteria, but also modify their environment [1]. Improvements in shutter, filter wheel and motorized stage speeds have accelerated the acquisition process. The introduction of brighter fluorescent proteins and dyes [36] has allowed investigators to greatly decrease exposure time with a consequent increase in cell viability under imaging conditions. These technological innovations have thus made deconvolution microscopy a more common tool. Deconvolution microscopy consists of acquiring a stack of images separated by a small interval (0.1 to 0.4 μm) in the *z*-axis. An algorithm based on the PSF (point spread function) of the optical system—the intensity profile created by a point—then uses a Fourier transform deconvolution function to deblur the images acquired.

In confocal microscopy, light is collected through a small pinhole to exclude out-of focus light as the sample is illuminated with a laser. The pinhole moves to scan the whole image. Laser intensity and pinhole size are critical variables of this system, as they determine both the signal-to-noise ratio and sample photobleaching. In a different configuration, spinning disk confocal microscopes use a disk with multiple holes that rotate to scan the whole image. The main throwback of this setup is that the pinhole is set to a unique size.

* Corresponding author. Tel.: +1 212 305 0316.
*E-mail address:* jed2113@columbia.edu (J. Dworkin).

0923-2508/$ - see front matter © 2007 Elsevier Masson SAS. All rights reserved.
doi:10.1016/j.resmic.2006.12.008

Although deconvolution microscopy does not use lasers as light sources, the acquisition is fast and the quality of its images is comparable to confocal microscopy without the associated sample bleaching. The recent introduction of spinning-disc confocal microscopes that do not depend on laser illumination may make the distinctions between the approaches more a matter of cost. Finally, although companies sell whole-packages of imaging systems, a background in optics, microscopy and programming greatly facilitates the use of such microscopes and the analysis of the rich and diverse data that can be obtained [30]. We will first describe the physical and biological basis necessary for usage of these microscopes and techniques.

### *1.2. Detecting protein interactions (FRET, BRET and BiFC)*

FRET occurs when a donor molecule is excited by a photon of a specific wavelength and transmits its energy through a non-radiative mechanism to the other molecule, the acceptor, which in turn looses its energy by emission of a fluorescent photon at a lower wavelength. The efficiency of this process has a strong $1/r^6$ dependence on the distance $r$ between the two molecules and is proportional to the spectral overlap between the emission spectrum of the donor and the absorption spectrum of the acceptor and the relative orientation of their dipole moments [11]. In BRET (bioluminescence resonant energy transfer), the donor photon is provided by a chemical reaction, and thus light excitation is not necessary.

Direct optical measurements are necessarily limited in resolution by the wavelength of light. Light diffraction blurs the spatial information and it is no longer possible to distinguish two points closer than half the wavelength of the light used for observation—around 250 nm for GFP. As biologists crave increasingly precise knowledge of the world inside the cells, techniques that go beyond the optical limit without affecting the cell are needed [4]. For cell biology, one would ideally want a technique that gives suboptical information on the localization of proteins inside the cell and also about the binding partners of such proteins, all this in a time-resolved manner and for many proteins. One of the most notable properties of FRET is that due to its $1/r^6$ dependence it can be used as a spectroscopic ruler [5,41] that has a higher resolution than the optical diffraction limit: Molecular interactions can be measured down to 1–10 nm, or up to 50 times more precise than the diffraction limit of light.

The folding properties of GFP permit its use as a tool to detect the interaction between two proteins using a technique called BiFC (biomolecular fluorescence complementation). To do so, GFP is cut in two halves, an N-terminal fragment and a C-terminal fragment, and each is fused to one of two proteins [25]. If these proteins interact, the two GFP pieces will be close enough to reconstitute the protein and hence produce fluorescence. Multicolor BiFC is a variant of this technique using different fluorescent protein (FP) colors. It allows the investigator to visualize the interaction of multiple protein complexes with spectrally different protein tags in a single cell [20].

Although BiFC has a better signal-to-noise ratio than FRET since a fluorescent signal is produced only if the proteins interact, the physical conditions for this interaction are not known and in some cases fluorescence is detected with non-interacting proteins [45]. Also, a higher level of protein expression can be sufficient for indiscriminate GFP complementation. Finally, the main caveats of this technique are its irreversibility and that GFP reconstitution can take up to 3000 s [20].

### *1.3. Measuring protein mobility*

Fluorescence recovery after photobleaching (FRAP) is used to assess the mobility or to obtain the diffusion coefficient of a fluorescence-emitting protein in cells. An area within the cell where the protein is present is photobleached, and then the time it takes to recover near to initial fluorescence levels is measured. This recovery is due to diffusion of proteins from non-photobleached areas, so it depends on the diffusion coefficient of the protein and the geometry of the system. Bleaching has to be performed with a brief pulse from a laser whose bleaching wavelength is equal to the fluorescence excitation. This is followed by the rapid acquisition of several images in the same focal plane to obtain the dynamics of the fluorescence changes within the bleached area. Due to the small size of bacteria, the laser spot needs to be the smallest possible ($\sim$0.7 μm), imposing an additional technical constraint on the measurement.

Various considerations have to be taken into account depending on the expected mobility of the protein. If fluorescence recovery takes more than 30 min, protein synthesis can play a major role. In this case, addition of a protein synthesis inhibitor like puromycin could be useful. Also, if the diffusion is too fast, the recovery time can be too short to be detected with current setups. For GFP, the smallest protein ($\sim$20 kDa) used for FRAP in vivo, this limit is not reached.

Calculating the diffusion coefficient involves transforming the two-dimensional image to a one-dimensional fluorescence intensity profile and then solving the one-dimensional diffusion equation. One has to consider illumination heterogeneities, initial distribution and geometry of the fluorescence. The diffusion coefficient will be given by the decay coefficient of the exponential that best fits the temporal change in intensity profile. A variant of this technique is to photoactivate a GFP variant that emits a 100-fold higher intensity after excitation with a 415 nm source [31]. In this case, the diffusion coefficient will be given by the time required for photoactivated molecules to diffuse out of the area where the laser was pointed for photoactivation. The advantage of this approach being that it has a better signal-to-noise ratio than FRAP because fluorescence is compared to the background.

## 2. GFP microscopy

We will now describe the biological applications of visualizing GFP signals in single bacterial cells.

### 2.1. Protein localization and dynamics

Determining the localization of a bacterial protein and following its spatial and temporal dynamics has generated significant insight into the molecular mechanisms underlying several fundamental biological phenomena. Among many examples, the observations of *Escherichia coli* MinD pole-to-pole dynamics [33], the helical localization of *Bacillus subtilis* MreB [7], and rapid subunit exchange in *E. coli* FtsZ rings [40] clearly illustrate the power of this approach. Here, instead of a comprehensive survey of the many applications of these techniques, we will focus on several examples that provide illustrations of their usefulness.

Gitai et al. monitored the segregation of different sites in the chromosome of *Caulobacter crescentus* by marking one site with a *lacO* array and the other site with a *tetO* array and expressing both LacI-CFP and TetR-YFP [13]. The ability to observe chromosome segregation in such detail allowed convincing demonstration that the origin region segregated via an MreB-dependent mechanism differently than the rest of the chromosome. In a study of the dynamics of a putative *B. subtilis* DNA repair enzyme, time-lapse movies showed that DisA-GFP scans the chromosome and pauses at sites where DNA lesions were created [3]. These kinds of approaches have also been used to study single molecules in vivo such as membrane-bound Tsr-YFP [44]. Here, the slow diffusion of membrane proteins permitted abrupt bleaching of the signal, which demonstrated that indeed single molecules were being detected.

Single molecule GFP detection was used to determine the number of molecules produced by transcriptional bursts and to study their stochastic nature when low numbers of transcripts were produced [6]. An alternative approach using a GFP fusion protein that tags mRNA identified a similar pattern of bursting [14]. Fluorescence correlation spectroscopy (FCS) has also been used to characterize in real time the activity of an *E. coli* promoter [23]. FCS measures the fluctuations of the fluorescent signal emitted by a low-concentration molecule (nanomolar range) in a small volume (femtomoliter range). While the molecule is in focus, fluctuations of its fluorescent signal due to interactions and conformational changes can be detected by autocorrelation of its fluorescence [16].

### 2.2. Detection of an active protein

While characterizing the subcellular spatial and temporal dynamics of an individual protein is useful, assaying its in vivo activity would add immeasurably to an understanding of its function. For example, if the protein is a kinase, determining when it phosphorylates its substrate or if it is a transcription factor, when it is binding its target DNA sequence would be very useful. A very simple and clever technique recently developed by Batchelor et al. [2] allows one to precisely do that. OmpR is part of the *E. coli* two-component signaling system EnvZ–OmpR that, when phosphorylated, binds to the *ompF* and *ompC* promoter sequences ($P_{ompF}$ and $P_{ompC}$). Using clustering multicopy plasmids with binding sites for OmpR, they demonstrated the presence of phosphorylated OmpR-YFP (P∼OmpR-YFP). They detected fluorescent clusters formed as P∼OmpR-YFP bound to $P_{ompF}$ and $P_{ompC}$ in these plasmids (see Fig. 1). By adding *lacO* sequences to the same plasmid, LacI-CFP served as a control indicating the localization of the multicopy plasmids in the cell. A post-translational modification in a protein leading to a specific DNA sequence (un)binding is sufficient for expanding this technique to other bacterial pathways.

### 2.3. Cell population heterogeneity

Isogenic bacteria can have heterogeneous behaviors and different responses to changes in the environment. Thus, monitoring isogenic cell populations over time and analyzing differences in single bacteria can lead to discovering new properties. The introduction of GFP has greatly advanced the understanding of heterogeneity, allowing both a more sophisticated analysis of the phenomenon and a growing understanding of the mechanisms underlying this heterogeneity.

An early example of GFP usage for measuring heterogeneity in a population of cells was the observation that at low levels of arabinose, only 1% of cells expressing $P_{araBAD}$-GFP were fluorescent [38], but 89% became fluorescent when high levels of arabinose were added. Arabinose-uptake transporters are expressed only when arabinose is present in the cell. Therefore, at low levels of induction, only a small percentage of cells that were stochastically expressing the uptake transporters became fluorescent. Another example of heterogeneity in a cell population was observed with *B. subtilis* under competence inducing conditions. Only 5–10% of the cells expressed the competence master regulator ComK fused to a GFP [15], providing an explanation for the previously observed inability to achieve a higher level of competence in the population. Süel et al. [42] more closely examined cell population heterogeneity by following the dynamics of the competence gene network. They followed a population of single cells through competence and sporulation and measured simultaneously the expression of different competence promoters fused to fluorescent proteins (Fig. 2C). They found that only ∼4% of the cells go into competence and of those cells, only ∼6% went through a second competence event, implying that competence events are stochastic and memoryless (Fig. 2D). Finally, in *B. subtilis* undergoing exponential growth, ∼20% of cells grew as chains, with the rest growing as single or double cells [19]. The alternative sigma factor $\sigma^D$ controls chaining and motility, and imaging $\sigma^D$ controlled GFP expression, revealed that only swarming cells are fluorescent (Fig. 2A,B). Although *swrA* expression, controlling flagellar genes, shifts the proportion towards more swarming cells, the mechanism underlying this bistable population is not yet understood.

Elowitz et al. [9] performed the first demonstration of inherent heterogeneities in isogenic bacterial populations. Genes encoding CFP and YFP under the control of identical promoters were inserted at equidistant sites from the origin of replication *oriC* in *E. coli*. Differences in CFP/YFP fluorescence

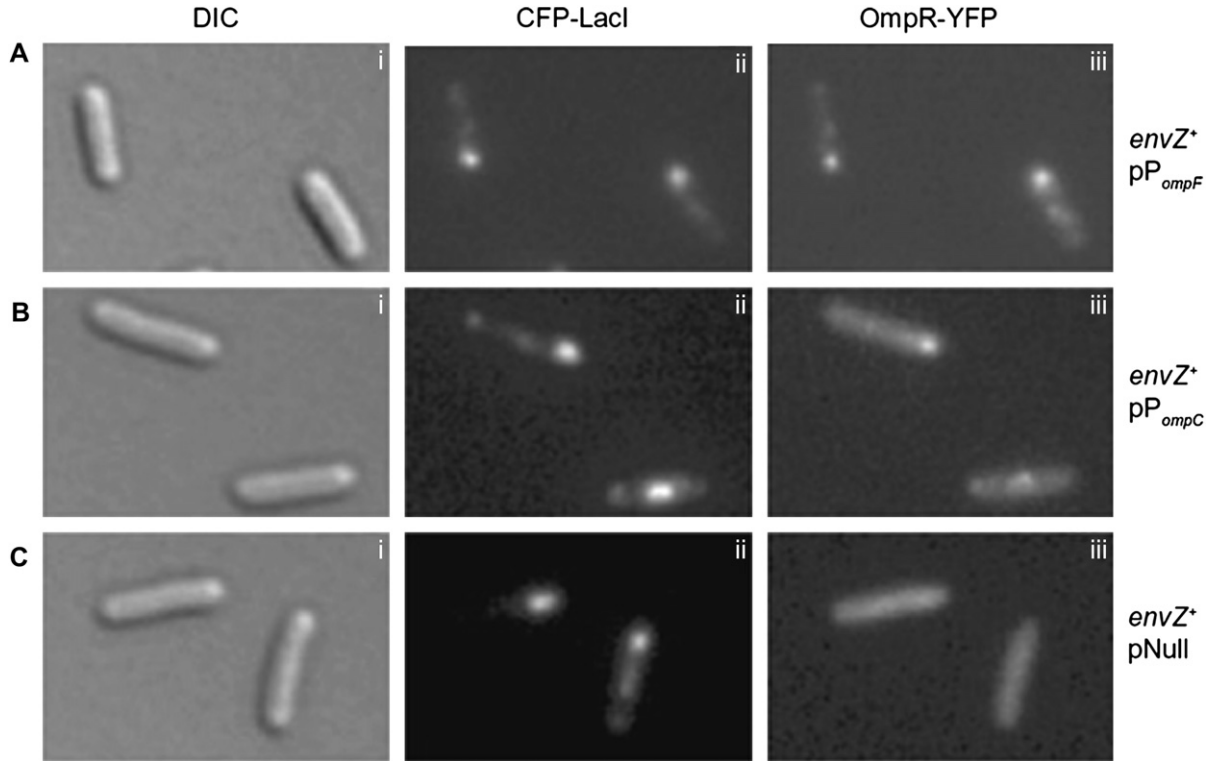


Fig. 1. Detecting kinase activity in single live cells. OmpR-YFP association with plasmid clusters containing *ompF* or *ompC* promoters. DIC (i), CFP (ii) and YFP (iii) images. (A) envZ+, plasmid with *ompF* promoter), (B) envZ+, plasmid with *ompC* promoter), (C) envZ+, control plasmid without *ompF* or *ompC* ). (courtesy E. Batchelor, M. Goulian and *Molecular Microbiology*.)

in a single cell were interpreted as a signature of the inherent stochastic processes of gene expression, or intrinsic noise, whereas differences in cell-to-cell expression levels were interpreted as a consequence of extrinsic noise. By comparing snapshots of cell populations, they found that intrinsic noise monotonically decreased with fluorescence expression levels. Extrinsic noise initially increased to a maximum and then also decreased with fluorescence expression levels. A fluorescent marker can hence be used to probe a population of cells and to generate precise and detailed information about the nature of this population.

## 3. Resonance energy transfer

We will now describe the more technically demanding technique based on the phenomenon of FRET to measure in vivo protein–protein interactions.

### *3.1. FRET*

A simple approach to assay FRET is acceptor photobleaching. This technique relies on the fact that when FRET occurs, the donor emits less photons as it de-excites by transferring the energy directly to the acceptor. Thus, FRET results in an increase in donor fluorescence intensity if the acceptor is photobleached. The disadvantage of this technique is that the acceptor is irreversibly destroyed and it is not possible to obtain further FRET measurements in the same cell [35]. FRET can also be measured directly by quantifying the signal of the FRET channel and comparing it to CFP only expressing cells. For example, FRET levels in two populations of *B. subtilis* cells expressing fusions to the cold shock proteins CspB-CFP and CshB-YFP were compared with this method [18,21]. To inhibit transcription and disrupt the putative protein–protein interaction, rifampin was added and the change in the FRET signal was measured.

The setup for measurements of CFP/YFP ratios in time-lapse experiments is simple to implement as just two filter cubes are needed for acquisition, one for the CFP and one for the YFP image. One caveat is that both CFP and YFP signals have to be large and of the same order of magnitude in order to obtain a high signal-to-noise ratio and avoid the preponderance of random variations typically seen in time-lapse experiments. An example of this approach is analysis of the CheY-YFP/CheZ-CFP interaction in response to addition and subtraction of chemo-attractants in *E. coli* [39]. Measurements of CFP/YFP ratios were performed seconds apart, which allowed following the dynamics of CheY/CheZ interactions with high temporal precision although no spatial data was obtained.

At first glance, the method of subtracting the bleed-through contributions seems to be indirect and tortuous. However, in practice, the actual process is not that difficult. One has to subtract from the image obtained with the donor (here CFP) excitation filter and acceptor (here YFP) emission filter, the weighted images taken with the CFP filters, and the image

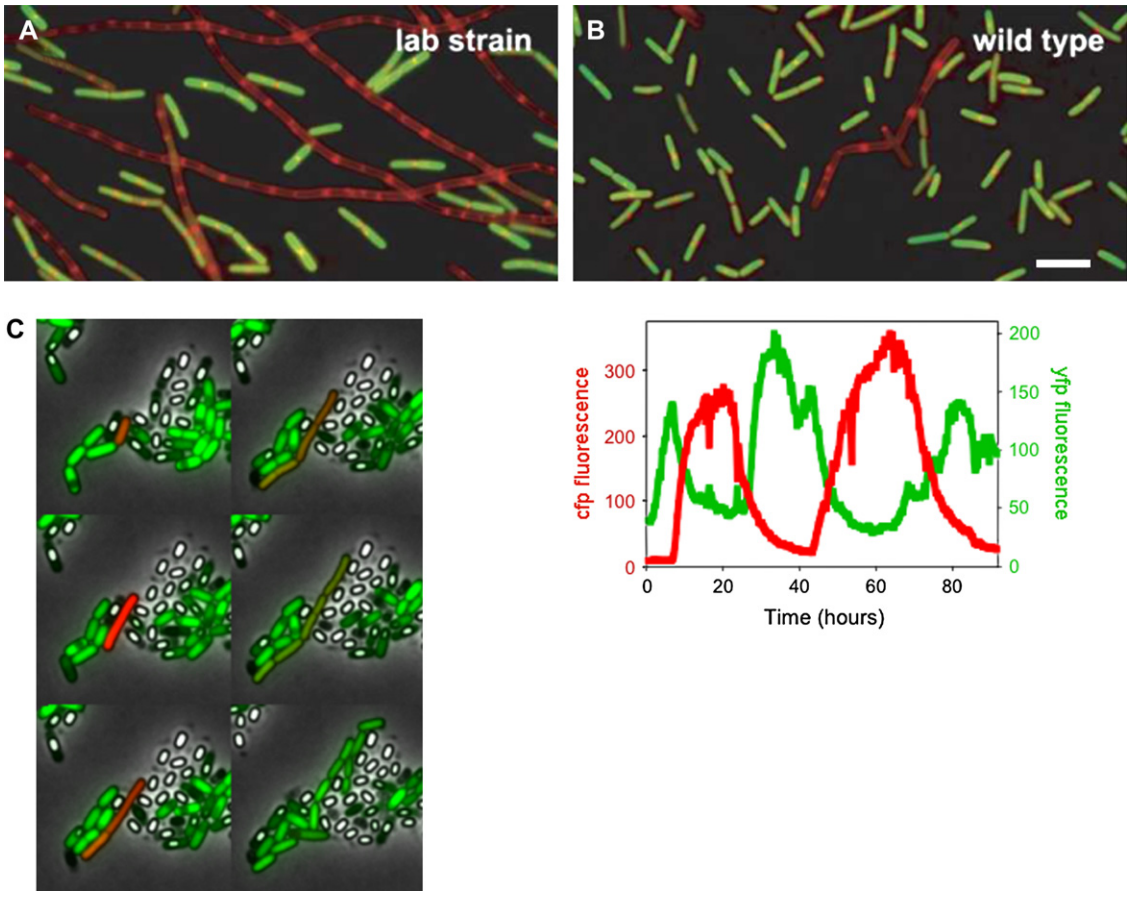


Fig. 2. Observing heterogeneity in cell populations. (A,B) Differences in heterogeneity between wild type and laboratory strains. Swarming cells express $P_{hag}$–GFP (green), where *hag* is the structural $\sigma^D$ controlled-gene for the flagellar filament. Membranes were stained with FM4-64 (red). (courtesy D.B. Kearns and R. Losick from *Genes & Development*.) (C) Heterogeneity of *B. subtilis* cells in sporulation media. Frames from film footage of a typical competence event with $P_{comS}$–yfp and $P_{comG}$–cfp expression shown in green and red, respectively. Note phase bright cells denoting completely formed spores. Time after beginning of sporulation is indicated in hours. (D) Quantitative time traces of consecutive competence events within a single cell lineage. $P_{comS}$ and $P_{comG}$ are anti-correlated during competence. Colors same as in (C). (C, D courtesy of Gürol Suël.)

obtained with the YFP filters. The weighted coefficients are previously calculated in samples expressing only CFP or only YFP and the investigator must be careful as they may vary with the fluorescence intensity. It is also necessary to normalize in order to compare different time points of a same cell or of different cells. This normalization also implies that CFP and YFP intensities are of the same order of magnitude (~20% difference), as a big difference would give rise to a nonsensical measure. Further developments of this method can lead to calculations of the stoichiometry of the proteins in complex [17]. This approach makes use of a complementary FRET technique called FLIM (fluorescence lifetime imaging) that measures the increased lifetime of the donor-fluorophore when it interacts with the acceptor molecule.

Several analyses of FRET dynamics have been reported. Interactions between the phosphatase PleC-YFP and response regulator DivK-CFP at the swarm pole of *C. crescentus* [26] were monitored by FRET in single cells at different times during the cell cycle. A somewhat different approach was taken with *E. coli*, where cells were immobilized in a flow chamber and cycled through additions of chemo-attractants and buffer (Fig. 3). Changes in localization and interactions of the phosphatase CheZ-CFP and the kinase CheY-YFP were monitored in the same cell by FRET [43]. Addition of chemoattractant caused substantially larger phosphatase activity at CheY-YFP clusters than in the cytoplasm. This clustering created a gradient of P~CheY in the cytoplasm, implying that motors proximal to the cluster would spin clockwise and motors distal to the cluster would spin counterclockwise.

As illustrated by these experiments, FRET is best used to measure changing rather than static interactions. Photobleaching can give a simple initial clue about the existence of an interaction. Then, the ideal situation for measuring FRET at various time points is to perform time-lapse experiments in single cells where the protein–protein interaction varies over time. This strategy eliminates fluctuations due to cell variability, and optimizes relative FRET measurements.

### 3.2. BRET

BRET is commonly implemented between *Renilla* luciferase (RLuc) and YFP, as RLuc emission spectrum is similar

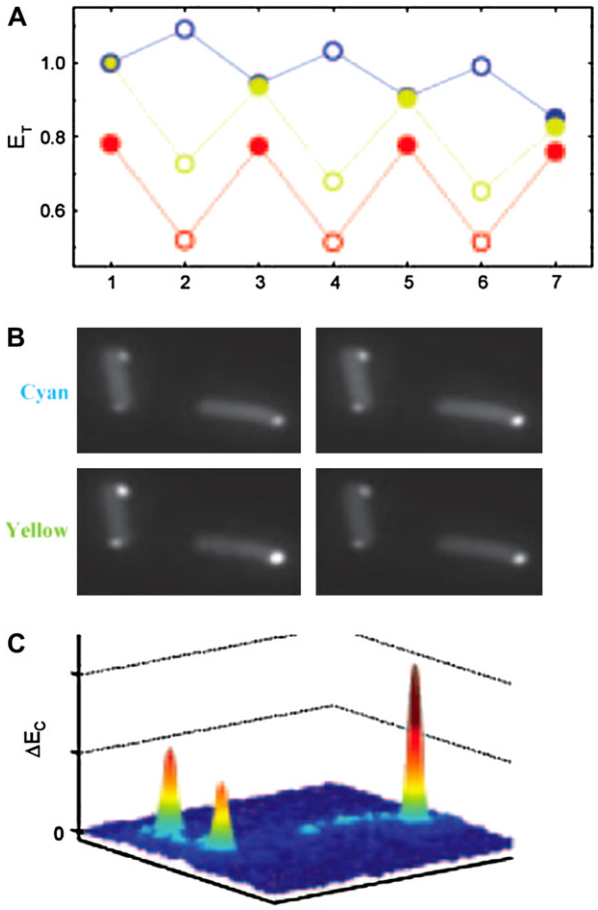


Fig. 3. FRET measurement of interactions between CheY-YFP and CheZ-CFP in *E. coli*. Addition of attractant abolishes CheY/CheZ interactions. (A) The total emission ($E_T$) in the cyan (blue) and the yellow (yellow) channels, and their ratio (red) in buffer (filled symbols) or attractant (open symbols). (B) Spatial distributions of the emission intensity in the cyan and yellow channels for the same cells in buffer (left) or attractant (right). (C) The spatial distribution of the change in the cyan emission ($\Delta E_C$), i.e., the emission in attractant minus that in buffer. As FRET disappears with attractant addition, CFP fluorescence is higher. (Courtesy of A. Vaknin, H.C. Berg and *PNAS*.)

to CFP. RLuc/YFP ratio was used to measure BRET between CheZ-RLuc/CheY-YFP [37]. The advantage of RLuc/YFP as compared to CFP/YFP is the absence of auto-fluorescence and phototoxicity due to excitation. *E. coli* is sensitive to blue light and stops swimming when exposed to it for long intervals. Shimizu et al. thus showed that absence of feedback from the flagellar motor when jammed by antibodies did not affect levels of P∼CheY, measured as CheZ-RLuc/CheY-YFP interactions. A caveat of this approach is that RLuc has a dimmer signal than CFP and thus photomultipliers and long exposures (10 s to 40 s) are needed to obtain a bright YFP signal. For the same reason it is not possible to obtain subcellular spatial information from BRET experiments in bacteria. Nevertheless, recent progress has been performed for intra-neuronal calcium imaging [34] using aequorin (containing coelenterazine, a luciferin-like chromophore) coupled to GFP as a reporter of calcium influx and it is possible that such approaches could be adapted for use in bacteria.

## 4. Protein mobility

FRAP can be used to precisely measure protein diffusion coefficients [8,10,29], or to obtain a qualitative assay of protein mobility [24,26,27].

### *4.1. Reversible photobleaching*

The *B. subtilis* SpoIIIE protein is required for chromosome translocation across the sporulation septum and thus likely forms a transient pore between the mother cell and the forespore. Liu et al. [24] used FRAP to show that GFP diffuses from the mother cell into the forespore in *B. subtilis ΔspoIIIE* cells (Fig. 4A). To demonstrate this, they bleached free GFP in the forespore for 50 ms with a 488 nm Argon laser, then imaged every 15 s and observed recovery of fluorescence. A second example using reversible photobleaching measured the reappearance of DivK-GFP in FtsZ-depleted filamentous *C. crescentus* cells after photobleaching one pole for 5 s, showing that DivK interactions at the poles are dynamic [26]. Induction of cytokinesis by expression of FtsZ inhibits this recovery, presumably through suppression of DivK dynamism after cytokinesis. In a very interesting study, Mignot et al. [27] showed that *Myxococcus xanthus* FrsZ-GFP moves from one pole to the other to form new type IV pili as the direction of movement is reversed. As the new pilus is being formed, both cells poles have FrsZ-GFP clusters. By photobleaching FrsZ-GFP for 10 s with a laser at one of the poles they showed that the recovery of fluorescence takes up to 40 s and concluded that FrsZ-GFP does not move by free diffusion around the cell but directionally with a speed less than 0.3 μm/s.

### *4.2. Measuring diffusion coefficients*

Elowitz et al. [10] and Mullineaux et al. [29] measured the diffusion coefficients of free GFP in *E. coli* in more quantitative studies requiring the fitting of the fluorescent intensity profiles to a single decaying exponential. Elowitz et al. obtained $7.7 \pm 2.5$ μm$^2$/s for free diffusing GFP by scanning every 300 ms after a 500 ms laser pulse, and similarly, Mullineaux et al. obtained $9 \pm 2.1$ μm$^2$/s by scanning every 4 s after a 3 s laser pulse. Taking these studies one step further, a recent experiment measured the change in GFP diffusion coefficient in *E. coli* as a function of osmotic stress (Fig. 4B) [22]. As the osmotic pressure rose, GFP freely diffused until a threshold was reached and its diffusion coefficient decreased abruptly. The putative causes for this observation could be increased viscosity of the cytoplasm, binding of GFP, molecular crowding effects or confinement within the cytoplasmic meshwork. Finally, in *B. subtilis*, Cowan et al. [8] found that the diffusion coefficient of free GFP in germinating spores was 4 orders of magnitude higher than in dormant spores, and they suggested that this resulted from the low water content of spores.

One can also apply these techniques to GFP-protein fusions. Mullineaux et al. measured diffusion coefficients for periplasm-associated Tar-GFP and membrane-associated

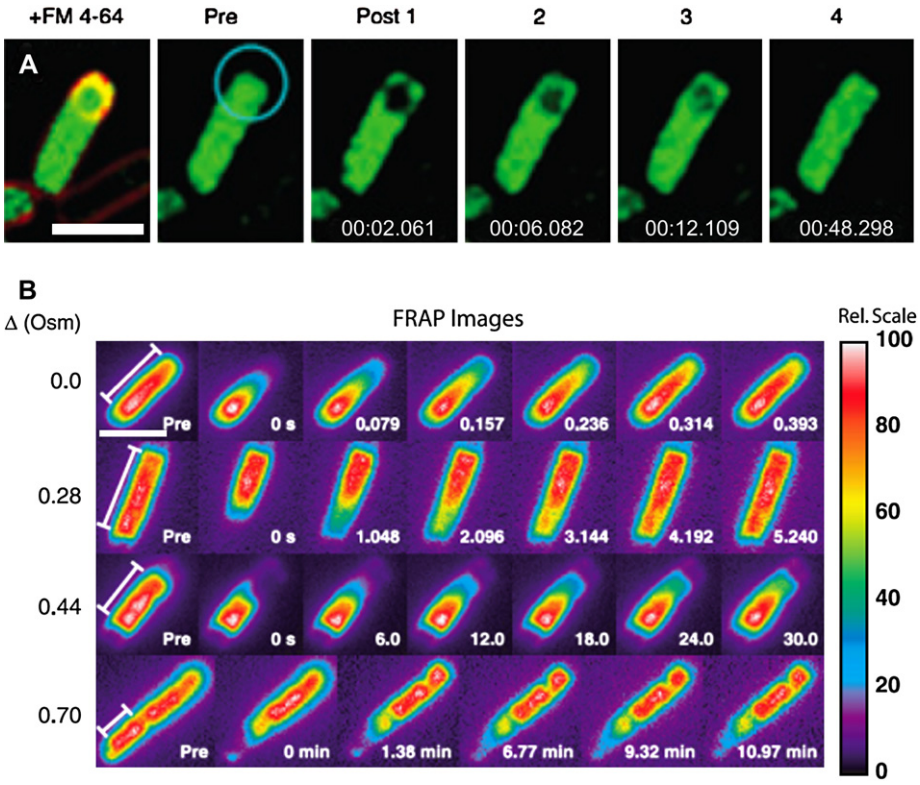


Fig. 4. FRAP measurements in *B. subtilis* and *E. coli* cells. (A) *B. subtilis* cells expressing CotE-GFP were harvested at t3 of sporulation and stained with FM 4-64. The regions indicated by aqua circles were irreversibly bleached with subsequent images collected as quickly as possible. Times are shown as min.s.ms. In the fusion-defective mutant, the forespores of sporangia with GFP in both cells were bleached. Immediately after photobleaching (Post 1), GFP diffused back into the slender arms of mother cell cytoplasm around the forespore. In contrast, GFP slowly diffused into the forespore within 45–90 s. (Courtesy of Liu et al. and *Molecular Microbiology*.) (B) Sequences of FRAP images for *E. coli* cells grown in 0.24 osmolal LB (Osm) and shifted as shown. The intensity scale is renormalized to 100 for each image. The prebleach (Pre) image and subsequent times are indicated. Bar: 2 μm. (Courtesy of Konopka et al. and *Journal of Bacteriology*.)

TatA-GFP, as $0.13 \pm 0.03$ μm$^2$/s and $2.6 \pm 1.2$ μm$^2$/s respectively. This study demonstrated quantitatively the result that membrane-associated GFP is quasi-immobile and that periplasmic GFP is almost 5 times slower than free GFP.

An alternative approach to assaying protein mobility was used to study LamB distribution and dynamics in *E. coli* [12]. LamB localizes to the outer membrane and is responsible for maltose uptake and acts as a receptor for phage lambda. Fluorescently labeled lambda phage tails interacting with LamB were used to probe LamB localization. A helical distribution of LamB around the cell was observed. Also, the movement of lambda phage bound to a gold particle was tracked and two populations of LamB were found, one mobile and one immobile. This clever technique enables to study protein distributions and dynamics on the outer cell membrane, a site difficult to reach with common fluorescent tools.

## 5. Discussion and future directions

The observation that some proteins exhibit patterns of subcellular localization in bacteria has prompted a wide interest in fluorescence imaging. Globally, the imaging techniques that have been developed for eukaryotic cells are transferable to bacteria. Although the small size of bacteria complicates experiments, in practice, the limit is set by the intensity of the fluorescent signal measured. Finally, the ease and simplicity of bacterial genetic manipulations greatly facilitates the design of fluorescence imaging experiments.

FRET has become a very popular technique, which is perhaps somewhat surprising due to its inherent technical difficulties and the flurry of non-standardized methods. An important take-home message of this review is that FRET changes are much easier to detect through time-lapse microscopy of single cells than comparison of different cells under different conditions.

Although somehow technically demanding, the techniques described here should receive increasingly broad acceptance in the microbiological community as a component of the experimenter's toolkit. In the not too distant future, these complementary techniques may resolve the details, from transcription to the protein dynamics, of a single signaling or metabolic pathway. This could lead to answering the question posed by Schrödinger in his seminal 1943 essay, *What is Life?*:

> "How can the events in space and time which take place within the spatial boundary of a living organism be accounted for by physics and chemistry?"

## Acknowledgments

We thank Nicolas Minc and Alison North for comments on the manuscript.

## References

[1] N.Q. Balaban, et al., Bacterial persistence as a phenotypic switch, Science 305 (5690) (2004) 1622–1625.
[2] E. Batchelor, M. Goulian, Imaging OmpR localization in *Escherichia coli*, Mol. Microbiol. 59 (6) (2006) 1767–1778.
[3] M. Bejerano-Sagie, et al., A checkpoint protein that scans the chromosome for damage at the start of sporulation in *Bacillus subtilis*, Cell 125 (4) (2006) 679–690.
[4] E. Betzig, et al., Imaging intracellular fluorescent proteins at nanometer resolution, Science 313 (5793) (2006) 1642–1645.
[5] M.E. Bowen, et al., Single-molecule studies of synaptotagmin and complexin binding to the SNARE complex, Biophys. J. 89 (1) (2005) 690–702.
[6] L. Cai, N. Friedman, X.S. Xie, Stochastic protein expression in individual cells at the single molecule level, Nature 440 (7082) (2006) 358–362.
[7] R. Carballido-Lopez, J. Errington, A dynamic bacterial cytoskeleton, Trends Cell Biol. 13 (11) (2003) 577–583.
[8] A.E. Cowan, et al., A soluble protein is immobile in dormant spores of *Bacillus subtilis* but is mobile in germinated spores: implications for spore dormancy, Proc. Natl. Acad. Sci. USA. 100 (7) (2003) 4209–4214.
[9] M.B. Elowitz, et al., Stochastic gene expression in a single cell, Science 297 (5584) (2002) 1183–1186.
[10] M.B. Elowitz, et al., Protein mobility in the cytoplasm of *Escherichia coli*, J. Bacteriol. 181 (1) (1999) 197–203.
[11] R.H. Fairclough, C.R. Cantor, The use of singlet-singlet energy transfer to study macromolecular assemblies, Methods Enzymol. 48 (1978) 347–379.
[12] K.A. Gibbs, et al., Complex spatial distribution and dynamics of an abundant *Escherichia coli* outer membrane protein, LamB, Mol. Microbiol. 53 (6) (2004) 1771–1783.
[13] Z. Gitai, et al., MreB actin-mediated segregation of a specific region of a bacterial chromosome, Cell 120 (3) (2005) 329–341.
[14] I. Golding, et al., Real-time kinetics of gene activity in individual bacteria, Cell 123 (6) (2005) 1025–1036.
[15] B.J. Haijema, et al., A ComGA-dependent checkpoint limits growth during the escape from competence, Mol. Microbiol. 40 (1) (2001) 52–64.
[16] E. Haustein, P. Schwille, Single-molecule spectroscopic methods, Curr. Opin. Struct. Biol. 14 (5) (2004) 531–540.
[17] A. Hoppe, K. Christensen, J.A. Swanson, Fluorescence resonance energy transfer-based stoichiometry in living cells, Biophys. J. 83 (6) (2002) 3652–3664.
[18] K. Hunger, et al., Cold-induced putative DEAD box RNA helicases CshA and CshB are essential for cold adaptation and interact with cold shock protein B in *Bacillus subtilis*, J. Bacteriol. 188 (1) (2006) 240–248.
[19] D.B. Kearns, R. Losick, Cell population heterogeneity during growth of *Bacillus subtilis*, Genes Dev. 19 (24) (2005) 3083–3094.
[20] T.K. Kerppola, Visualization of molecular interactions by fluorescence complementation, Nat. Rev. Mol. Cell. Biol. 7 (6) (2006) 449–456.
[21] D. Kidane, P.L. Graumann, Intracellular protein and DNA dynamics in competent *Bacillus subtilis* cells, Cell 122 (1) (2005) 73–84.
[22] M.C. Konopka, et al., Crowding and confinement effects on protein diffusion in vivo, J. Bacteriol. 188 (17) (2006) 6115–6123.
[23] T.T. Le, et al., Real-time RNA profiling within a single bacterium, Proc. Natl. Acad. Sci. USA. 102 (26) (2005) 9160–9164.
[24] N.J. Liu, R.J. Dutton, K. Pogliano, Evidence that the SpoIIIE DNA translocase participates in membrane fusion during cytokinesis and engulfment, Mol. Microbiol. 59 (4) (2006) 1097–1113.
[25] T.J. Magliery, et al., Detecting protein–protein interactions with a green fluorescent protein fragment reassembly trap: scope and mechanism, J. Am. Chem. Soc. 127 (1) (2005) 146–157.
[26] J.Y. Matroule, et al., Cytokinesis monitoring during development; rapid pole-to-pole shuttling of a signaling protein by localized kinase and phosphatase in *Caulobacter*, Cell 118 (5) (2004) 579–590.
[27] T. Mignot, J.P. Merlie Jr., D.R. Zusman, Regulated pole-to-pole oscillations of a bacterial gliding motility protein, Science 310 (5749) (2005) 855–857.
[28] I. Mihalcescu, W. Hsing, S. Leibler, Resilient circadian oscillator revealed in individual cyanobacteria, Nature 430 (6995) (2004) 81–85.
[29] C.W. Mullineaux, et al., Diffusion of green fluorescent protein in three cell environments in *Escherichia coli*, J. Bacteriol. 188 (10) (2006) 3442–3448.
[30] A.J. North, Seeing is believing? A beginners' guide to practical pitfalls in image acquisition, J. Cell Biol. 172 (1) (2006) 9–18.
[31] G.H. Patterson, J. Lippincott-Schwartz, A photoactivatable GFP for selective photolabeling of proteins and cells, Science 297 (5588) (2002) 1873–1877.
[32] D.C. Prasher, et al., Primary structure of the *Aequorea victoria* green-fluorescent protein, Gene 111 (2) (1992) 229–233.
[33] D.M. Raskin, P.A. de Boer, MinDE-dependent pole-to-pole oscillation of division inhibitor MinC in *Escherichia coli*, J. Bacteriol. 181 (20) (1999) 6419–6424.
[34] K.L. Rogers, et al., Visualization of local Ca2+ dynamics with genetically encoded bioluminescent reporters, Eur. J. Neurosci. 21 (3) (2005) 597–610.
[35] R.B. Sekar, A. Periasamy, Fluorescence resonance energy transfer (FRET) microscopy imaging of live cell protein localizations, J. Cell Biol. 160 (5) (2003) 629–633.
[36] N.C. Shaner, P.A. Steinbach, R.Y. Tsien, A guide to choosing fluorescent proteins, Nat. Methods 2 (12) (2005) 905–909.
[37] T.S. Shimizu, et al., Monitoring bacterial chemotaxis by using bioluminescence resonance energy transfer: absence of feedback from the flagellar motors, Proc. Natl. Acad. Sci. USA. 103 (7) (2006) 2093–2097.
[38] D.A. Siegele, J.C. Hu, Gene expression from plasmids containing the araBAD promoter at subsaturating inducer concentrations represents mixed populations, Proc. Natl. Acad. Sci. USA. 94 (15) (1997) 8168–8172.
[39] V. Sourjik, H.C. Berg, Receptor sensitivity in bacterial chemotaxis, Proc. Natl. Acad. Sci. USA. 99 (1) (2002) 123–127.
[40] J. Stricker, et al., Rapid assembly dynamics of the *Escherichia coli* FtsZ-ring demonstrated by fluorescence recovery after photobleaching, Proc. Natl. Acad. Sci. USA. 99 (5) (2002) 3171–3175.
[41] L. Stryer, Fluorescence energy transfer as a spectroscopic ruler, Annu. Rev. Biochem. 47 (1978) 819–846.
[42] G.M. Suel, et al., An excitable gene regulatory circuit induces transient cellular differentiation, Nature 440 (7083) (2006) 545–550.
[43] A. Vaknin, H.C. Berg, Single-cell FRET imaging of phosphatase activity in the *Escherichia coli* chemotaxis system, Proc. Natl. Acad. Sci. USA. 101 (49) (2004) 17072–17077.
[44] J. Yu, et al., Probing gene expression in live cells, one protein molecule at a time, Science 311 (5767) (2006) 1600–1603.
[45] S. Zhang, C. Ma, M. Chalfie, Combinatorial marking of cells and organelles with reconstituted fluorescent proteins, Cell 119 (1) (2004) 137–144.